ELSEVIER

Journal of Chromatography A, 683 (1994) 279–291

JOURNAL OF CHROMATOGRAPHY A

Second-order kinetics in the liquid chromatographic reactor

Richard Thede[a], Detlef Haberland[a], Zengqun Deng[b], Stanley H. Langer[b,*]

[a]*Department of Chemistry, University of Greifswald, Soldtmannstrasse 23, D-17489 Greifswald, Germany*

[b]*Department of Chemical Engineering, University of Wisconsin, 1415 Johnson Drive, Madison, WI 53706-1691, USA*

First received 31 March 1994; revised manuscript received 31 May 1994

Abstract

Equations for the determination of second order rate constants with the pulse overlay method, based on the application of empirical peak shape equations are derived. This approach was then applied in an experimental study of the rection of pyridine with tetrachloroterephthaloyl chloride in a reversed-phase HPLC system. Rate constants evaluated from reaction chromatograms were found to be in good agreement with those obtained earlier for this reaction by Chu and Langer in chromatographic reactor experiments under pseudo-first order conditions.

1. Introduction

Chromatographic reactors can provide a number of advantages for carrying out and studying chemical reactions [1–5]. The determination of rate constants through analysis of typical reaction chromatograms from chemical reactions in chromatographic columns has been described by many workers over the last three decades for gas chromatographic systems and, more recently, for liquid chromatographic systems. A number of reviews and references to other reviews on these subjects are available [1–5]. However, almost all the published applications and theoretical work have been devoted to first-order or pseudo-first-order reactions which were either reversible or irreversible.

Up to the end of the last decade there were only two papers [6,7] describing second-order reaction studies on gas chromatographic columns; in both instances numerical evaluations of the rate constant were used. More recently, the concept of the "extended ideal chromatographic reactor (EICR)" [8,9] was proposed and applied to second-order reactions on gas chromatographic columns, simplifying the calculations for obtaining rate constants to a considerable extent. For the EICR development the following assumptions are used: (1) isothermal column, negligible temperature and pressure gradients neglected, (2) linear sorption isotherms, (3) rate of mass transfer does not limit the chemical reaction, (4) the reactant peak shape is a Gaussian function, (5) the first absolute moment and the second central moment depend linearly on the local coordinate.

Assumptions 1–3 coincide with those of the "ideal chromatographic reactor" model introduced by Langer and co-workers [4,5]. Assumptions 4 and 5 which extend this model with respect to peak shape and peak spreading are necessary for treating second-order reactions.

The EICR model, however, has the character of an "ad hoc hypothesis", and it was somewhat

* Corresponding author.

0021-9673/94/$07.00
SSDI 0021-9673(94)00512-8

unclear, how it might fit within the framework of the original balance equations of the chromatographic reactor. The purpose of this work is to explore the connection between these models and, moreover, to report some results from an initial experimental investigation of a second-order reaction in a liquid chromatographic reactor.

2. Mathematical modeling

2.1. Balance equations

We can start the theoretical treatment with the balance equations of isothermal linear chromatographic systems, which are commonly considered sufficient [10] for modeling the chromatographic process, and extend them with general reaction terms. (More sophisticated models which have been discussed, i.e. [11], are more suitable for the elucidation of partition kinetics than for our purposes.)

For concentration in the mobile (m) phase:

$$D_i \cdot \frac{\partial^2 c_i}{\partial x^2} - \frac{\partial c_i u}{\partial x} - k_{fi} q_i c_i + k_{fi} a_{si} + r_{mi} = \frac{\partial c_i}{\partial t} \tag{1a}$$

For concentration in the stationary (s) phase:

$$k_{fi} q_i c_i - k_{fi} a_{si} + r_{si} = \frac{\partial a_{si}}{\partial t} \tag{1b}$$

These balance equations can be simplified further by neglecting diffusional effects (which is justified for liquid chromatography in general and for gas chromatography with adequate flow-rates) and addressing situations where mass transfer rates do not limit reaction kinetics. Then,

$$-\frac{\partial c_i u}{\partial x} - k_{fi} q_i c_i + k_{fi} a_{si} - r_i = \frac{\partial c_i}{\partial t} \tag{2a}$$

$$k_{fi} q_i c_i - k_{fi} a_{si} = \frac{\partial a_{si}}{\partial t} \tag{2b}$$

The "lumped" reaction term r_i is the sum of the reaction terms r_{mi} and r_{si} considering the effective phase volume ratios of the mobile phase and the stationary phase with the kinetic time variable. The latter can be the void time or the reactant retention time or, where more than one reactant is involved, each of the reactant retention times. With first-order reactions the retention time of the reactant is generally used. For second-order reactions we can reference with respect to the void time, since then results can be interrelated where more than one reactant with different retentions are involved. The general reaction term, r_i, is then

$$r_i = \sum_{j=1}^{m} \nu_{ij} k_{aj} \prod_{i=1}^{l} c_i^{\alpha_{ij}} \tag{3}$$

with the apparent rate constant of the jth reaction:

$$k_{aj} = k_{mj} + \frac{V_s}{V_m} \cdot k_{sj} \prod_{i=1}^{l} K_i^{\alpha_{ij}} \tag{4}$$

Now, the partial differential equation system (2) can be transformed into a system of ordinary differential equations of the statistical moments of the reactants through multiplication of the whole system (2) by t^0 for the zeroth moment, t^1 for the first moment, t^2 for the second moment and so on, followed by integrating the system over time from zero to infinity. Using the defining equations for the moments, a tedious but straightforward rearrangement leads to the following set of ordinary differential equations for the zeroth absolute and the first four moments:

$$\left.\begin{aligned}
&-u \cdot \frac{\mathrm{d} \ln \bar{m}_{0i}}{\mathrm{d}x} = m_{R0i} \\
&-u \cdot \frac{\mathrm{d}\mu_{1i}}{\mathrm{d}x} + (q_i + 1) = u \cdot \frac{\mathrm{d} \ln \bar{m}_{0i}}{\mathrm{d}x} \cdot (\mu_{1i} - \mu_{R1i}) \\
&-u \cdot \frac{\mathrm{d}\mu_{2i}}{\mathrm{d}x} + 2\left[\mu_{1i}(q_i + 1) + \frac{q_i}{k_{fi}}\right] \\
&\quad = u \cdot \frac{\mathrm{d} \ln \bar{m}_{0i}}{\mathrm{d}x} \cdot (\mu_{2i} - \mu_{R2i}) \\
&-u \cdot \frac{\mathrm{d}\mu_{3i}}{\mathrm{d}x} + 3\left[\mu_{2i}(q_i + 1) + 2 \cdot \frac{q_i \mu_{1i}}{k_{fi}} + 2 \cdot \frac{q_i}{k_{fi}^2}\right] \\
&\quad = \frac{\mathrm{d} \ln \bar{m}_{0i}}{\mathrm{d}x} \cdot (\mu_{3i} - \mu_{R3i}) \\
&-u \cdot \frac{\mathrm{d}\mu_{4i}}{\mathrm{d}x}
\end{aligned}\right\} \tag{5}$$

$$+4\left[\mu_{3i}(q_i+1)+3\cdot\frac{q_i\mu_{2i}}{k_{fi}}+6\cdot\frac{q_i\mu_{1i}}{k_{fi}^2}+6\cdot\frac{q_i}{k_{fi}^3}\right]$$

$$=u\cdot\frac{\mathrm{d}\ln\bar{m}_{0i}}{\mathrm{d}x}\cdot(\mu_{4i}-\mu_{R4i})$$

An arbitrary formulation for any moment is found to be:

$$-u\cdot\frac{\mathrm{d}\mu_{ni}}{\mathrm{d}x}+n\left[\mu_{(n-1)i}(q_i+1)+\sum_{j=2}^{n}\frac{(n-1)!}{(j-2)!}\frac{q_i\mu_{(j-2)i}}{k_{fi}^{n+1-j}}\right]=u\cdot\frac{\mathrm{d}\ln\bar{m}_{0i}}{\mathrm{d}x}\cdot(\mu_{ni}-\mu_{Rni}) \quad (6)$$

It can be noted that the derivation of Eq. 5 does not require the introduction of any simplifications. Furthermore, in these formulae the linear flow-rate, u, is still a function of the local coordinate, x. Therefore, a zeroth moment was introduced, which is related to the average flow-rate in a chromatographic column. For a gas chromatographic column the flow-rate, u, is usually obtained from the relation

$$u=\frac{l}{t_0}\cdot\frac{p^3-1}{p^2-1}\cdot\frac{1}{\sqrt{p^2-(p^2-1)\frac{x}{l}}} \quad (7)$$

For a liquid chromatographic system, however, with negligible mobile phase compressibility and constant linear flow-rate, the zeroth moment itself can be used.

2.2. Introduction of empirical peak shape equations

Eq. 5 contains terms of the form, μ_{Rni}, designated as "moments of reaction". Those are abbreviations of the following:

$$\mu_{Rni}=\frac{\int_0^\infty r_i t^n\,\mathrm{d}t}{\int_0^\infty r_i\,\mathrm{d}t} \quad (8)$$

For irreversible reactions following simple power law kinetics, Eq. 8 in terms of concentrations becomes

$$\mu_{R_{ni}}=\frac{\int_0^\infty t^n\prod_{i=1}^{l}c_i^{\alpha_i}\,\mathrm{d}t}{\int_0^\infty\prod_{i=1}^{l}c_i^{\alpha_i}\,\mathrm{d}t} \quad (9)$$

Furthermore, these concentrations can be expressed in terms of a product of concentration–time (peak-) areas and distribution density (peak shape) functions:

$$c_i=m_{0i}\Psi_i \quad (10)$$

For such irreversible reactions, the moments of the reactions are the moments of the reaction order power of the peak shape functions:

$$\mu_{Rni}=\frac{\int_0^\infty t^n\prod_{i=1}^{l}\Psi_i^{\alpha_i}\,\mathrm{d}t}{\int_0^\infty\prod_{i=1}^{l}\Psi_i^{\alpha_i}\,\mathrm{d}t} \quad (11)$$

For first-order reactions, it can be seen that there is no difference between the moments of reaction and the common moments. Therefore, the differences in Eq. 5 become zero to give a linear differential equation system. However, to evaluate the reaction moments for a second order reaction the peak shapes which are solutions of Eq. 2 appear to be necessary. Fortunately there are empirical and plausible peak shape functions, which might be used in place of the unknown solutions. Of these, the Gaussian function is the simplest and most frequently encountered.

2.3. Reaction Type, $2A_1 \rightarrow P$

For simplicity, a dimerization reaction can be considered first. For this reaction type we examine besides the Gaussian, the EMG function [12], the Gram–Charlier series (GCS) [13] and the GEX function [14] as well. (Function representations are given in the list of symbols.)

Analytical solutions are available for GCS and for the Gaussian, of course, with the framework of Eq. 11. They are presented here in terms of central moments, beginning with the second, because of simpler formulations. (Any set of

central moments can be converted into a set of absolute moments and vice versa.)

For the Gaussian function (with only one reactant, the index i can be omitted):

$$\left.\begin{aligned} m_{R0} &= \frac{m_0^2}{2\sqrt{\pi\mu_2'}} \\ \mu_{R1} &= \mu_1 \\ \mu_{R2}' &= \frac{\mu_2'}{2} \\ \mu_{R3}' &= 0 \\ \mu_{R4}' &= \frac{3}{4}\cdot\mu_2'^2 \end{aligned}\right\} \quad (12)$$

For the GCS (Note that the μ_{Rn}' are central moments over μ_1, not over μ_{R1}):

$$\left.\begin{aligned} m_{R0} &= \frac{m_0}{2\sqrt{\pi\mu_2'}}\left[1+\frac{5S^2}{96}+\frac{E}{16}+\frac{35E^2}{3072}\right] \\ \mu_{R1} &= \mu_1 + \frac{\frac{5ES}{384}-\frac{S}{4}}{\frac{35E^2}{3072}+\frac{E}{16}+\frac{5S^2}{96}+1} \\ \mu_{R2}' &= \frac{\mu_2'}{2}\left[\frac{\frac{25E^2}{1024}-\frac{3E}{16}+\frac{11S^2}{96}+1}{\frac{35E^2}{3072}+\frac{E}{16}+\frac{5S^2}{96}+1}\right] \\ \mu_{R3}' &= \frac{\frac{11ES}{256}-\frac{S}{8}}{\frac{35E^2}{3072}+\frac{E}{16}+\frac{5S^2}{96}+1} \\ \mu_{R4}' &= \frac{3\mu_2^2}{4}\cdot\left[\frac{1+\frac{163E^2}{3072}-\frac{13E}{48}+\frac{25S^2}{96}+1}{\frac{35E^2}{3072}+\frac{E}{16}+\frac{5S^2}{96}+1}\right] \end{aligned}\right\} \quad (13)$$

The other peak shape equations apparently do not permit an analytical solution with respect to Eq. 11. However, the possibility of fitting a linear regression model to the numerical results of Eq. 11 remains. Using the Gaussian shape as an ideal model, the differences between the moments of the reaction for the Gaussian and for the other peak shape equations can be considered:

$$\left.\begin{aligned} F_0(\mu_{R0},\mu_i,\mu_2') &= \frac{2\sqrt{\pi\mu_2'}m_{R0}}{m_0^2}-1 \\ F_1(\mu_{R1},\mu_i,\mu_2') &= \frac{\mu_{R1}-\mu_1}{\sqrt{\mu_2'}} \\ F_3(\mu_{R3},\mu_i,\mu_2') &= \frac{\mu_{R3}'}{\sqrt{\mu_2'^3}} \\ F_4(\mu_{R4},\mu_i,\mu_2') &= \frac{4\mu_{R4}'}{3\mu_2'^2}-1 \end{aligned}\right\} \quad (14)$$

Using results from Eq. 12 in the equations above it can be seen that all F_i values become zero for Gaussian shapes. To match the deviations of the other functions from the Gaussian the following regression model can be used:

$$F_i(\mu_{Ri},\mu_i,\mu_2') = a_{1i}S + a_{2i}E + a_{3i}S^2 + a_{4i}E^2 + a_{5i}SE \quad (15)$$

Results from those regressions are summarized in Table 1. Eq. 5 was solved using a fourth-order Runge–Kutta method. All of the empirical peak shape equations give fairly similar plots when this is done for moments vs. the local coordinate (see Fig. 1). Table 2 shows that the results for the GCS are in increasing accord with the solution of Eq. 2 by an explicit finite difference method as the number of grid points in the length coordinate increases.

Table 3 illustrates some results for a com-

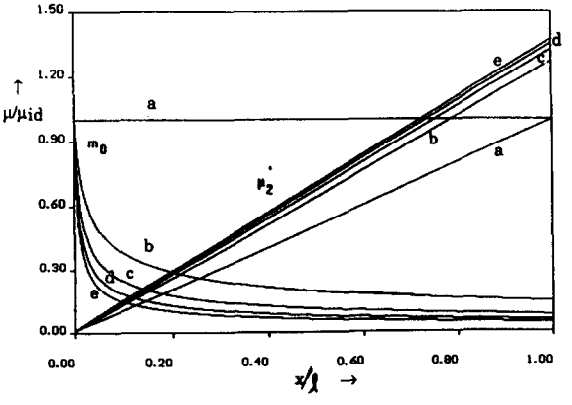

Fig. 1. Increase of the second central moment of the reactant with increasing conversion (reduced moments referenced to values without reaction) and advancement through the column. Conversions: a = 0%; b = 85%; c = 90%; d = 93%; e = 96%.

Table 1
Coefficients for deviations from Gaussian function for empirical peak shape equations calculated from Eq. 15

F (EMG)	a_1	a_2	a_3	a_4	a_5
m_0	0.0387	0	0.0952	0	0
μ_1	−0.137	0	−0.0851	0	0
μ_2	−0.209	0	−0.0169	0	0
μ_3	0.0957	0	0.0897	0	0
F (GEX)	a_1	a_2	a_3	a_4	a_5
m_0	0	0.0444	0.0745	−0.0138	0
μ_1	−0.291	−0.0457	0.0703	0	0.0630
μ_2	0.0291	−0.246	0.147	0.193	0.114
μ_3	0.315	0.0922	−0.136	−0.0827	−0.186
μ_4	0	−0.395	0.565	0.264	0.298

Table 2
Comparison between the moments obtained from Eq. 11 with the GCS function and the results from a finite difference solution (FD) of Eq. 3 with increasing grid points ($q = 1$, $k_a = 1$, $m_0(0) = 1$, $k_f = 100$, $\mu_2'(0) = 0.001$, $x = 1$)

Number of points in x-direction	$\frac{m_0(\text{GCS})}{m_0(\text{FD})}$	$\frac{\mu_1(\text{GCS})}{\mu_1(\text{FD})}$	$\frac{\mu_2(\text{CS})}{\mu_2(\text{FD})}$	$\frac{\mu_3(\text{GCS})}{\mu_3(\text{FD})}$	$\frac{\mu_4(\text{GCS})}{\mu_4(\text{FD})}$
100	0.812	1.00	0.550	0.219	0.304
500	0.951	1.00	0.867	0.661	0.801
1000	0.977	1.00	0.936	0.830	0.914
7500	0.998	1	0.9997	0.963	0.975

parison between the empirical peak shape equations. The EMG function deviates most from results with the others. Results from use of the GEX function do not differ much from those using the GCS function. Therefore, from those considered here the GCS function is the next best approximation relative to the Gaussian.

The following conclusions results from this numerical investigation:

(1) The first absolute moment does not depend significantly on conversion.

(2) The second central moment increases with conversion, however its linear dependence on the locale coordinate is maintained.

(3) The deviation of the fourth central moment, or in other words of the excess, has the largest influence on non-ideal deviations with conversion.

Table 3
Comparison between the moments from the GCS and the other empirical functions using Eq. 11 (parameters: see Table 2, GAU = Gaussian)

Peak shape function (PSF)	$\frac{m_0(\text{GCS})}{m_0(\text{PSF})}$	$\frac{\mu_1(\text{GCS})}{\mu_1(\text{PSF})}$	$\frac{\mu_2(\text{GCS})}{\mu_2(\text{PSF})}$	$\frac{\mu_3(\text{GCS})}{\mu_3(\text{PSF})}$	$\frac{\mu_4(\text{GCS})}{\mu_4(\text{PSF})}$
GAU	1.001	1.004	0.986	–	–
EMG	1.007	1.001	0.971	0.848	–
GEX	1.003	1.0	0.996	0.978	1.005

The first conclusion above enables us now to derive the equations of the EICR from Eq. 5, i.e. from the balance equations, since in this case it becomes possible to rewrite Eq. 5 to yield:

$$\left.\begin{aligned} &-\frac{1}{u}\cdot m_{R0}=\frac{d\ln m_0}{dx}\\ &\frac{d\Delta\mu_1}{dx}=0\\ &\frac{d\Delta\mu_2'}{dx}=\frac{d\ln m_0}{dx}\cdot(\mu_{R2}'-\mu_2')\\ &\frac{d\Delta\mu_3'}{dx}=\frac{d\ln m_0}{dx}\cdot(\mu_{R3}'-\mu_3')\\ &\frac{d\Delta\mu_z'}{dx}+6\mu_2'\cdot\frac{d\Delta\mu_2'}{dx}=\frac{d\ln m_0}{dx}\cdot(\mu_{R4}'-\mu_4') \end{aligned}\right\} \quad (16)$$

The first three equations of Eq. 16 —together with the Gaussian assumption for the peak shape equation— are the very equations of the EICR, and for the case of a Gaussian model the other equations become non-relevant. The solution for this situation was presented in [15].

For the zeroth moment we find:

$$\frac{1}{m_0}=\frac{1}{m_0(0)}+\frac{2k_a t_0}{\sqrt{\pi\mu_2'}} \quad (17)$$

We can also find an equation for the zeroth moment using the GCS model, the first equation of the system (5), and a linear dependence of the second central moment on the local coordinate. However, the use of the GCS model results in realistic chromatographic peaks only in a limited range, for the skew and for the excess. If the second central moment of the injected peak becomes very small, as assumed for the EICR, the skew and the excess produced by Eq. 2 become very large. Therefore, the introduction of the GCS model as the "next best approximation" to the real chromatographic peak demands well defined initial conditions. Fortunately, the availability of injection valves with a well defined geometry with liquid chromatography makes this problem less challenging than with gas chromatography.

2.4. Reactions of the type, $A_1 + A_2 \rightarrow P$

This reaction type is at first glance considerable more complicated, since one has to deal with the moments of both reactants and the distance between them in space and in time, since in most instances the chromatographic process will give separation because of the differences in the rate of travel of these peaks through the column. Thus, no simple regression model could be found, and the theoretical investigation of peak shape equations had to be confined to these cases of analytical solution of Eq. 11 where Gaussian and GCS peak shapes were involved. The analytical solutions of the moments of the reaction with the GCS could only be obtained in a compact form using the following terms:

$$\left.\begin{aligned} &\int_0^\infty \Psi_1\Psi_2 t^n\,dt\\ &\quad=\int_{-\infty}^{\infty}\frac{1}{\sqrt{2\pi(\mu_{21}'+\mu_{22}')}}\cdot e^{-\frac{(\mu_{11}-\mu_{12})^2}{2(\mu_{21}'+\mu_{22}')}}\\ &\quad\cdot\frac{1}{\sqrt{2\pi}\sigma_0}\cdot e^{-\frac{1}{2}\cdot\frac{\xi^2}{\sigma_0^2}}f_1(\xi-\mu)\cdot f_2\left(\frac{\xi+\sigma^2\mu}{\sigma}\right)\\ &\quad\cdot\sqrt{\mu_{21}'^n}\xi^n\,d\xi\\ &\sigma^2=\frac{\mu_{22}'}{\mu_{21}'}\\ &\mu=\frac{\mu_{id}-\mu_{11}}{\sqrt{\mu_{21}'}}\\ &\mu_{id}=\frac{\mu_{22}'\mu_{11}+\mu_{12}'\mu_{21}}{\mu_{21}'+\mu_{22}'}\\ &\sigma_0^2=\left(\frac{\mu_{21}'\mu_{22}'}{\mu_{21}'+\mu_{22}'}\right)\cdot\frac{1}{\mu_{21}'}\\ &f_i(z)=\frac{S_i}{6}(z^3-3z)+\frac{E_i}{24}\cdot(z^4-6z^2+3) \end{aligned}\right\} \quad (18)$$

Since these solutions require several pages they are not presented here. Now, we are again able to apply the Runge–Kutta method to the solution of system 11 and thereby investigate the moments as functions of the local coordinate.

As illustrated in Figs. 2 and 3 the use of GCS as the "next best approximation" relative to a Gaussian model results in a considerable deviation from the linear dependence of the second central moment on the local coordinate starting at conversions close to 50%. The initial conditions are of less importance for reaction type, since reaction can be initiated deeper into the

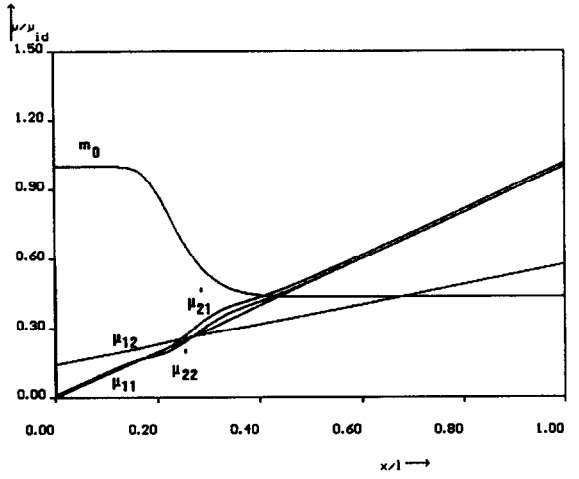

Fig. 2. Slight non-linearity in the second central moments in the case of a pulse overlay reaction with ca. 60% conversion (stoichiometric case, reduced moments referenced to values without reaction).

column, where well defined peak shapes are formed as a result of the chromatographic process with unreacted materials.

As shown before [16] for a linear dependence of the second central moments on the local coordinate, the following equations for the zeroth moment can be derived:

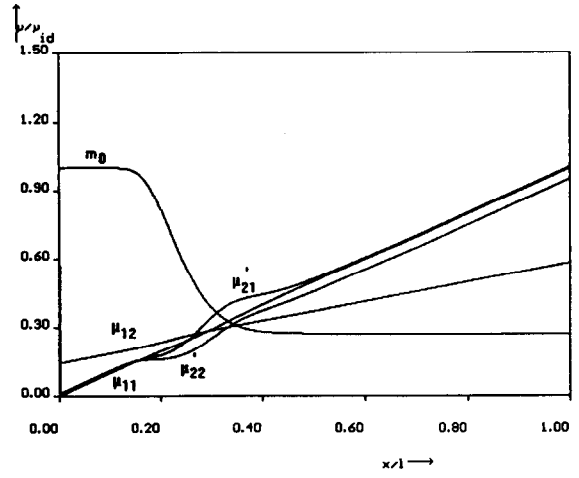

Fig. 3. Strong deviation from linearity in the second central moments in the case of a pulse overlay reaction with ca. 80% conversion (stoichiometric case, reduced moments referenced to values without reaction).

Non-stoichiometric case:

$$\ln\left(\frac{m_{01}}{m_{02}}\right) = \ln\left(\frac{m_{01}(0)}{m_{02}(0)}\right) + (m_{01}(0) - m_{02}(0))k_a t_0 \cdot \int_0^1 \frac{1}{\sqrt{2\pi(\mu'_{21} + \mu'_{22})}} \cdot \exp - \frac{(\mu_{11} - \mu_{12})^2}{2(\mu'_{21} + \mu'_{22})} \cdot \mathrm{d}\frac{x}{l} \tag{19}$$

Stoichiometric case:

$$\frac{1}{m_{01}} = \frac{1}{m_{01}}(0) + k_a t_0 \cdot \int_0^1 \frac{1}{\sqrt{2\pi(\mu'_{21} + \mu'_{22})}} \cdot \exp - \frac{(\mu_{11} - \mu_{12})^2}{2(\mu'_{21} + \mu'_{22})} \cdot \mathrm{d}\frac{x}{l} \tag{20}$$

The integral appearing in Eqs. 19 and 20 can be separated in the following way:

$$\left.\begin{aligned} &\int_0^1 \frac{1}{\sqrt{2\pi(\mu'_{21} + \mu'_{22})}} \cdot \exp - \frac{(\mu_{11} - \mu_{12})^2}{2(\mu'_{21} + \mu'_{22})} \cdot \mathrm{d}\frac{x}{l} \\ &= \frac{1}{\sqrt{(\mu_{11}(l) - \mu_{12}(l))^2}} \\ &\cdot \int_{-\infty}^{1-\Delta t' \cdot \sqrt{\frac{(\mu_{11}(l)+\mu_{12}(l))^2}{\mu'_{21}(l)+\mu'_{22}(l)}}} \frac{1}{\sqrt{(2\pi)}} \cdot \mathrm{e}^{-\frac{\xi^2}{2}} \mathrm{d}\xi \\ &+ \frac{1}{2} \cdot \int_0^1 \frac{1}{\sqrt{2\pi(\mu'_{21}(l) + \mu'_{22}(l))}} \cdot \frac{x - \Delta t'}{x} \\ &\cdot \mathrm{e}^{-\frac{(\mu_{11}(l)-\mu_{12}(l))^2}{\mu'_{21}(l)+\mu'_{22}(l)} \frac{(x-\Delta t')^2}{2x}} \mathrm{d}\frac{x}{l} \end{aligned}\right\} \tag{21}$$

where

$$\Delta t' = \frac{\Delta t}{|\mu_{11}(l) - \mu_{12}(l)|}$$

In those situations where the faster peak completely overtakes the slower one in the column, the first integral in Eq. 21 obviously will become unity and the second approach zero. Therefore, fairly simple equations become available for the zeroth moment:

Non-stoichiometric case:

$$\ln\left(\frac{m_{01}}{m_{02}}\right) = \ln\left(\frac{m_{01}(0)}{m_{02}(0)}\right) + (m_{01}(0) - m_{02}(0))k_a \cdot \frac{t_0}{|\mu_{11} - \mu_{12}|} \tag{22}$$

Stoichiometric case:

$$\frac{1}{m_{01}} = \frac{1}{m_{01}(0)} + k_a \cdot \frac{t_0}{|\mu_{11} - \mu_{12}|} \quad (23)$$

2.5. Evaluation of rate constants from experimental results

The calculation of rate constants from experiments minimally requires a knowledge of the following parameters: (a) flow-rate, (b) molar inlet amounts of reactants, (c) retention times of reactants and (recommended) void time, (d) standard deviation of reactant peak for the case $2A \rightarrow P$, (e) ratio of the outlet pulse area to the inlet pulse area for at least one of the reactants as measured for several different injection amounts (recommended) and/or flow-rates.

The last parameter is the most crucial, because chromatographic equipment generally does not allow a direct measurement of the inlet pulse area without an additional detector. However, the use of the following approaches makes it possible to proceed without the reactant area at the column inlet [4]:

(a) Internal standard method: an inert substance is mixed with one of the reactants, and the ratio of the pulse areas of both substances is measured in a non-reactive system. Then, for the reactive system this known ratio can be used to substitute for the inlet pulse area.

(b) Product-reactant method: where the ratio of the molar detector responses for the reactant and the product are known, then the loss of reactant area can be evaluated from the product area.

(c) External standard method: the difference between the external and the internal standard method is that the inert standard is not mixed with the reactant but introduced with a precision injector between reaction experiments. For the case of a reaction of the type $A_1 + A_2 \rightarrow P$, one of the reactants can serve as an external standard. This simplifies the calculations considerably.

Now, with the experimental parameters mentioned above rate constants can be obtained through: (I) numerical analysis from Eq. 2, (II) numerical analysis from Eq. 5, (III) analytically from Eqs. 17, and 22 or 23, respectively. As shown before, the results of method II will not differ significantly from method I, if a GCS function and appropriate initial conditions are applied. The time for the calculations however is considerably shorter with method II. In those situations where only moderate (up to 50–60%) conversions are achieved with equipment which is not particularly sophisticated, experimental error most probably will exceed the systematic error from use of the analytical equations.

The experimental system which was used to test the application of the equations above was the first step in the reaction of pyridine with tetrachloroterephthaloyl chloride ($TCTPCl_2$) shown below [17].

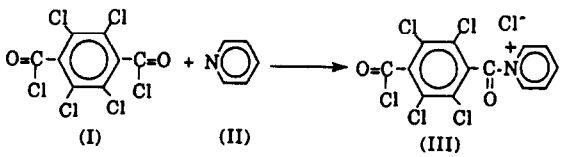

Addition of pyridine to tetrachloroterephthaloyl chloride: This well studied addition reaction to form a quaternary ammonium salt has been used earlier on a number of occasions as a model pseudo-first-order reaction [17,18] in the liquid chromatographic reactor. In the earlier experiments, pyridine was maintained in large excess in the mobile phase with pulses of $TCTPCl_2$ introduced into the liquid phase so that reaction could proceed as shown in Eq. 24. For testing the approach to the pulse overlay technique developed here, the reaction was carried out under conditions which made it truly second order.

3. Experimental

The array consisted of a Waters 590 HPLC pump, Beckman Model 210 sample injection valve with a 20-μl sample loop column, a Perkin-Elmer LC 55 variable-wavelength UV detector set at 275 nm and an SP 4050 Spectra-Physics

integrator. The column was Altex Ultrasphere ODS 250 mm × 4.6 mm I.D. Methanol (in glass-distilled grade) was the mobile phase.

A series of preliminary experiments was used to match the concentration conditions of a true second order reaction and to accommodate the limited solubility of $TCTPCl_2$ in methanol while achieving a reasonable conversion. With the wavelength and conditions used here a useful reaction chromatogram for both reactants (which have considerably different absorption characteristics in the UV range) and product was obtained.

Useful results were achieved using constant injections of $TCTPCl_2$ (0.05 *M* dissolved in tetrahydrofuran). Pyridine pulse concentrations were varied in the range from 0.4 to 0.1 *M* in steps of 0.1 *M* with a 0.2 ml/min flow-rate of methanol mobile phase. The flow-rate was also varied in the range from 0.2 to 0.5 ml/min in steps of 0.1 ml/min. The reaction was carried out at ambient temperature in a controlled-temperature room (about 298 K).

The $TCTPCl_2$ pulse as the slower moving reactant was introduced first, at which time the integrator was started. After about 1 min the pyridine pulse was introduced. To obtain the conversion with respect to the initial $TCTPCl_2$ pulse, separate $TCTPCl_2$ pulses were introduced to the column periodically as an external standard. This was done before each reaction experiment. Pyridine pulses were also introduced separately in a non-reacting mode in order to obtain the characteristic retention time.

4. Results and discussion

Figs. 4–6 show a series of typical reaction chromatograms with increasing pyridine concentrations. In these chromatograms the pyridine (II), the product quaternary ammonium salt (III) and $TCTPCl_2$ (I) are eluted consecutively. Now, in order to be comparable with earlier work [17] an apparent rate constant for the column with respect to $TCTPCl_2$ was evaluated, using Eq. 22 in the following formulation:

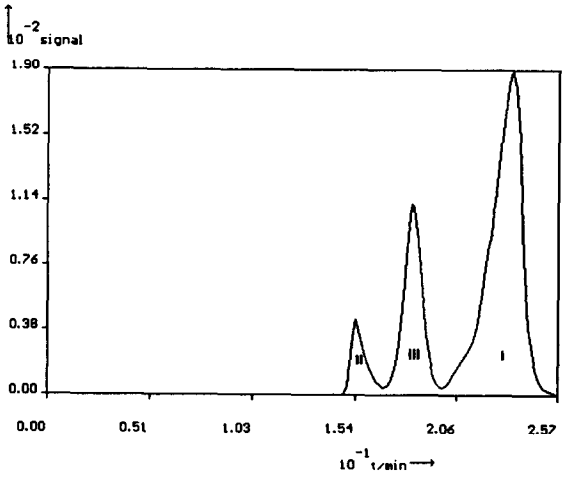

Fig. 4. Reaction chromatogram resulting from successive injections of $TCTPCl_2$ and pyridine (0.1 *M* pyridine). Peaks: II = pyridine; III = quaternary pyridinium salt; I = $TCTPCl_2$.

$$\left.\begin{aligned} X &= (c_{10} - c_{20}) \cdot \frac{20 \cdot 10^{-6} l}{\dot{v}} \\ Y &= \ln\left(\frac{A_1}{A_1(0)}\right) - \ln\left(1 + \frac{c_{10}}{c_{20}}\left(1 - \frac{A_1}{A_1(0)}\right)\right) \\ \text{and} \\ Y &= aX \end{aligned}\right\} \quad (24)$$

Index 1 refers to $TCTPCl_2$, with *A* representing

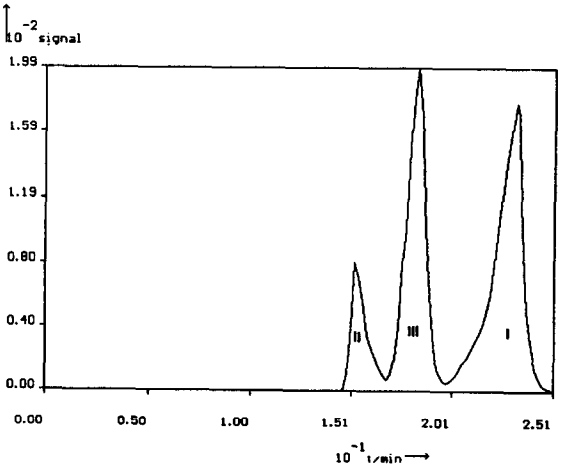

Fig. 5. Reaction chromatogram resulting from successive injections of $TCTPCl_2$ and pyridine (0.3 *M* pyridine). Peaks: II = pyridine; III = quaternary salt intermediate; I = $TCTPCl_2$.

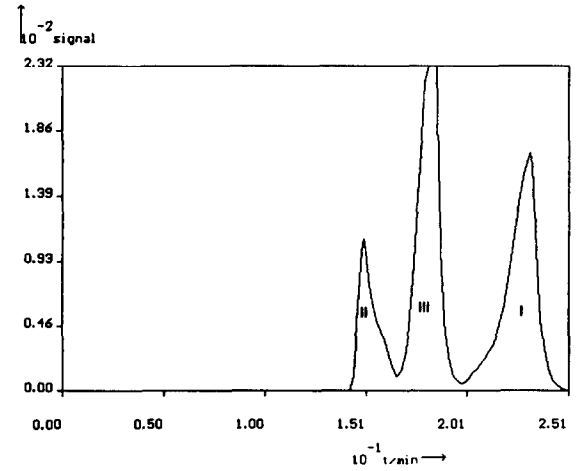

Fig. 6. Reaction chromatogram resulting from successive injections of $TCTPCl_2$ and pyridine (0.5 *M* pyridine). Peaks as in Fig. 5.

peak areas. The c_{10} and c_{20} are the concentrations of the pulsed solutions. The slope is then the product of the apparent rate constant for the column under our conditions and the corresponding time divided by the difference between reactant retention times. The intercept should be zero. Table 4 summarizes our results.

As can be seen, there is no significant difference between the slopes, and the intercepts do not significantly deviate from zero. Fig. 7 presents all the data of Table 4 in a single plot so that comparisons can be made.

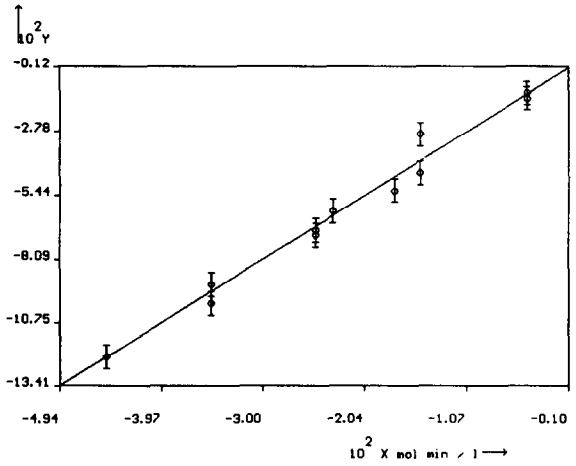

Fig. 7. Plot of *X* and *Y* of Eq. 24 for the $TCTPCl_2$–pyridine reaction.

From the slope of 2.78 ± 0.12 l/(mol · min) and the average ratio of the retention time difference 0.37 to the retention time of $TCTPCl_2$ we obtain an apparent second order rate constant of the reaction $k_a = 0.0171 \pm 0.0007$ l/(mol · s), which is in very good agreement with the rate constants, recalculated from our earlier pseudo-first order reaction constant measurements [17]: 0.019 l/(mol · s) (with 0.005 *M* pyridine) and 0.0177 l/(mol · s) (with 0.0075 *M* pyridine).

Moreover, it was possible to calculate a reaction chromatogram from Eq. 3. The molar detector responses could be calculated on the basis of material introduced to the column and measured chromatographic areas. The partial differential equation system was solved by an explicit finite difference method, using a grid of 1000 steps in space and time. The mass transfer coefficients were adjusted to meet the standard deviations of the pulses in a manner similar to the method used by Czok and Guiochon [19]. The resulting, calculated chromatogram is compared to an experimental one as shown in Fig. 8. Though there is some nonideality evident particularly for the $TCTPCl_2$-peak and there appears to be some interaction between the pyridine and the quaternary ammonium product, the agreement between these two chromatograms is quite satisfactory.

5. Conclusions

The peak overlay method offers the possibility of studying second-order reactions in the liquid chromatographic reactor even where retentions of the two reactants differ. In comparison to pseudo-first-order methods, it can offer advantages especially for fast reactions and also because there is the possibility of separating products and reactants completely.

To calculate the column rate constant, measurements of both reactant retention times and the peak area of one reactant is necessary. The Gram–Charlier series proved to be suitable for use as an empirical peak shape equation, how-

Table 4
Results from regressions of experimental values with respect to Eq. 24

Experiment (see Experimental section)	Slope $\left(\frac{\text{mol} \cdot \text{min}}{\text{l}}\right)$	Intercept
(1) Pyridine concentration varied	2.78 ± 0.19	$4.25 \cdot 10^{-3} \pm 5.41 \cdot 10^{-3}$
(2) Pyridine concentration varied	2.88 ± 0.09	$6.85 \cdot 10^{-3} \pm 2.20 \cdot 10^{-3}$
(3) Mobile phase flow-rate varied	2.79 ± 0.48	$-5.17 \cdot 10^{-4} \pm 1.26 \cdot 10^{-2}$

ever with moderate conversions the assumption of a Gaussian distribution is sufficient and leads to analytical terms for the evaluation of the rate constant. Experimental and numerical analysis showed that the rate constants found with this approach do not differ from those found by previously employed pseudo-first-order methods.

Since all the substances involved in reaction here can be —at least in principle— completely separated, a comparison of experimental with recalculated chromatograms is quite feasible, the latter requiring only experimentally observed rate constants and mass transfer coefficients. Further development of the approach described here should make it possible to broaden the application of the liquid chromatographic reactor in the study of reaction kinetics.

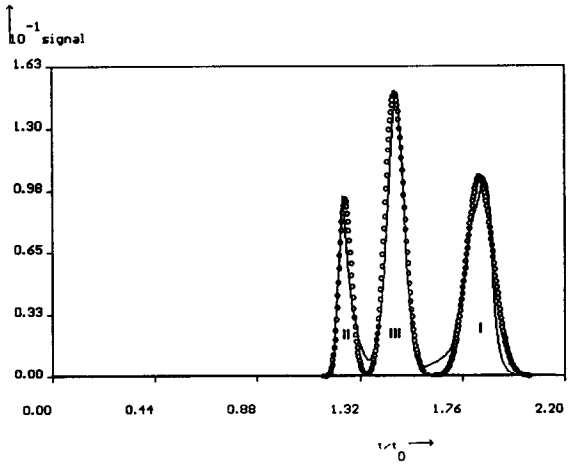

Fig. 8. Comparison of observed chromatogram with a numerically calculated chromatogram using a finite difference method (reduced time referenced to the column void time).

Symbols

A	Peak area
a_s	effective concentration in the stationary phase
c	concentration in the mobile phase
D	diffusion coefficient
E	excess of peak shape: $E = \frac{\mu_4' - 3\mu_2'^2}{\mu_2'^2}$
F_i	see Eq. 14
K	partition coefficient
k_f	mass transfer coefficient
k_a	apparent rate constant
k_s	rate constant (stationary phase)
k_m	rate constant (mobile phase)
l	length of the column
m_0	zeroth moment: $m_0 = \int_0^\infty c \, dt$
$m_0(0)$	zeroth moment at the column inlet
m_{R0}	zeroth moment of the reaction: $m_{R0} = \int_0^\infty r \, dt$
p	pressure
q	retention capacity
r	reaction terms
S	skew of peak shape: $S = \frac{\mu_3'}{\mu_2'^{3/2}}$
t	time
t_0	void time
u	linear flow-rate
v	volume or effective volume
$\dot{v}$	volume flow-rate
x	length coordinate
z	argument of the GCS (see Eq. 18)
α	partial reaction order

Δt time delay from the beginning of the measurements

$\Delta\mu$ difference between moment in reaction and without reaction

μ_n absolute nth moments:

$$\mu_n = \frac{\int_0^\infty t^n c \, dt}{m_0}$$

μ_n' absolute central moments:

$$\mu_n' = \frac{\int_0^\infty (t-\mu_1)^n c \, dt}{m_0}$$

μ_{id} absolute moments in case that no reaction occurs

μ_z' fourth semi-invariant: $\mu_z' = \mu_4' - 3\mu_2'^2$

μ_{Rn} nth moment of the reaction (Eq. 8)

$\mu(l)$ moment at the column outlet

ν stoichiomeric coefficient

ξ integration variable in Eq. 18 defined as

$$\xi = \frac{t-\mu_{id}}{\sqrt{\mu_{21}'}}$$

Ψ peak shape equation

GAU $$\Psi = \frac{1}{\sqrt{2\pi\mu_2'}} e^{-\frac{(t-\mu_1)^2}{2\mu_2'}}$$

GCS $$\Psi = \frac{1}{\sqrt{2\pi\mu_2'}} e^{-\frac{z^2}{2}}\left(1 + \frac{S}{6}(z^3 - 3z) + \frac{E}{24}(z^4 - 6z^2 + 3)\right)$$

$$z = \frac{t-\mu_1}{\sqrt{\mu_2'}}$$

EMG $$\Psi = \frac{1}{\tau}\exp\left(\frac{1}{2}\cdot\frac{\sigma_g^2}{\tau^2} - \frac{t-t_g}{\tau}\right)\int_{-\infty}^{\frac{t-t_g}{\iota\sqrt{2}}} e^{-\xi^2} d\xi$$

t_g breakthrough time of pulse maximum

σ_g width parameter

τ skew parameter

GEX $$\Psi = \frac{h_m}{m_0}\cdot\left(\frac{t-t_1}{t_g-t_1}\right)^{b-1} \cdot \exp\left(\frac{b-1}{a}\cdot\left[1 - \left(\frac{t-t_1}{t_g-t_1}\right)^a\right]\right)$$

h_m maximum peak height

t_1 break through time of pulse beginning

a, b shape parameters

Subscripts

i number of the substance

j number of the reaction

n number of the moment

m mobile phase

s stationary phase

Acknowledgement

We are grateful to the German Academic Exchange Service (DAAD) for their support of this work through a travel grant (to R.T.). We also appreciate support through the University of Wisconsin and help from Hazelton Laboratories of Madison through Mr. Robert L. Pesselman.

References

[1] R.J. Laub and R.L. Pecsok, *Physicochemical Applications of Gas Chromatography*, Wiley, New York, 1978.

[2] J.R. Conder and C.L. Young, *Physicochemical Measurements by Gas Chromatography*, Wiley, New York, 1979.

[3] G. Ganetsos and P.E. Barker (Editors), *Preparative and Process Scale Chromatographic Processes and Applications*, Marcel Dekker, New York, 1993.

[4] S.H. Langer and J.E. Patton, in J.H. Purnell (Editor), *New Developments in Gas Chromatography*, Wiley, New York, 1973, p. 293.

[5] C.Y. Jeng and S.H. Langer, *J. Chromatogr.*, 589 (1992) 1.

[6] L.G. Harrison and Y. Koga, *J. Chromatogr.*, 52 (1970) 39.

[7] P. Schulz, *Anal. Chem.*, 47 (1975) 1979.

[8] R. Thede, E. Below, D. Haberland and H. Pscheidl, *J. Chromatogr.*, 520 (1990) 109.

[9] R. Thede, H. Pscheidl and D. Haberland, *Z. Phys. Chem. (Leipzig)*, 271 (1990) 471.

[10] J.A. Jönsson, *Chromatography: Theory and Basic Principles*, Marcel Dekker, New York, 1985.

[11] A. Jaulmes and C. Vidal-Madjar, *Adv. Chromatogr.*, 28 (1989) 1.

[12] M.S. Jeansonne and J.P. Foley, *J. Chromatogr. Sci.*, 29 (1991) 258.

[13] F. Dondi, A. Betti, G. Blo and C. Bighi, *Anal. Chem.*, 53 (1981) 496.

[14] R.A. Vaidya and R.D. Hester, *J. Chromatogr.*, 287 (1984) 231.

[15] R. Thede, E. Möller, H. Pscheidl and D. Haberland, *Z. Phys. Chem. (Leipzig)*, 271 (1990) 891.

[16] R. Thede, F. Nohmie, H. Pscheidl and D. Haberland, *Z. Phys. Chem. (Munich)*, 173 (1991) 87.
[17] A.H.T. Chu and S.H. Langer, *Anal. Chem.*, 58 (1986) 1617.
[18] M.W. Bolme and S.H. Langer, *J. Phys. Chem.*, 87 (1983) 3363.
[19] M. Czok and G. Guiochon, *Anal. Chem.*, 62 (1990) 189.